ECS Solid State Letters, **2** (8) R27-R30 (2013)
2162-8742/2013/2(8)/R27/4/$31.00 © The Electrochemical Society

Synthesis of ZnSe Quantum Dots Using a Continuous-Flow Microreactor and Their White Emission through Energy Transfer

Byoung-Hwa Kwon, Hyunki Kim, Youngsun Kim, Dongseok Kang, and Duk Young Jeon[z]

Department of Materials Science and Engineering, Korea Advanced Institute of Science and Technology, Yuseong-gu, Daejeon 305-701, Korea

We report a continuous-flow microreaction synthesis of ZnSe quantum dots (QDs) which are controllable in their emission from blue to white light. The emission of ZnSe QDs exhibits quantum confinement effect, which is adjusted by the flow rate of precursor solution. The ZnSe QDs' high concentration solution shows red-shifted emission in the blue region and strongly enhanced green-yellow emission from deep levels due to the inter-QD energy transfer, thereby exhibiting white color with CIE color coordinates of (0.33, 0.33). The red-shifted band-edge emission with longer decay time in the dense solution confirms that the energy is transferred efficiently between QDs.
 [DOI: 10.1149/2.005308ssl]

Manuscript submitted March 25, 2013; revised manuscript received April 29, 2013. Published June 4, 2013.

Semiconductor quantum dots (QDs) have been attractive because of their size-tunable optical properties and chemical stabilities for the last decades.[1] Due to their unique characteristic properties, QDs have been used in various applications including cell imaging, biosensor, light-emitting diode (LED) and solar cells.[2–5] In solution-processed optoelectronic devices, QDs should be assembled to form solid film by dip coating or spin casting. The uniform and crack-free layer composed of Pb chalcogenide QDs exhibited high quantum efficiency due to enhanced carrier extraction between QDs.[6] In a biomedical area, various biomolecules can be appended to the QD to allow for sensing and/or targeting of cellular receptors through energy transfer process.[2,3] Therefore, understanding of this energy transfer among QDs and its application are essential for the development of future technology.

For the utilization of QD-based materials and devices in our life, two obstacles should be solved: (1) cost-effective mass production, (2) selection of non-toxic materials. Previously, research on the synthesis of QDs was focused on batch process, but that is not an effective method for mass production.[7] Recently, scientists have focused on chemical synthesis using microfluidic reaction as a novel way of producing different types of nanomaterials with better yields and easy size controllability.[8] The microfluidic system in the production of QDs provides a precise control of the reaction conditions, including high heat and mass transfer, precise temperature control, high surface-to-volume ratio, efficient mixing, low reagent consumption and continuous production.[9] In addition, it is possible to achieve scale-up production through parallel integration. Secondly, most previously developed QDs were composed of Cd chalcogenide material which is known as a hazardous substance to cause serious health problems.[4] In order to overcome the material issues, scientists have focused on and researched ZnSe and InP QDs.[10,11] The ZnSe QDs exhibit high fluorescence in UV to blue range without any Class A heavy metal ions (cadmium, mercury and lead).[12] In addition, the green and red emission can be controlled by impurity doping and/or surface functionalization.[13,14]

In this work, we reported the synthesis of white light-emitting ZnSe QDs using a continuous-flow microreactor for the first time. As-prepared ZnSe QDs had both spherical and rod-like shape, and their structure was a combination of zinc blende (ZB) and wurtzite (WZ). They had strong blue excitonic emission and weak defect emission related to surface and lattice defects. In the case of high concentration of QDs dissolved in solution, they showed white light with CIE color coordinates of (0.33, 0.33) due to the enhancement of radiative defect emission by inter-QD ET process, so we investigated their luminescent properties and mechanism.

Materials and Method

Zinc acetate (99.99%), selenium (100 mesh, 99.999%), 1-octadecene (ODE, 95%), oleylamine (OLA, technical grade), and octadecylamine (ODA, technical grade) were purchased from Aldrich. Tributylphosphine (TBP, technical grade) was purchased from TCI. The Zn precursor solution was prepared by heating Zn acetate (0.07 g, 0.4 mmoL) with OLA (0.4 mL, 1.2 mmoL) around 170 °C until the solution turned clear. For the Se precursor solution, Se powder (0.05 g, 0.6 mmoL) was dissolved in 1.0 mL of TBP to form the transparent solution and then ODA powder (0.05 g, 0.2 mmoL) was dissolved in that mixture, and finally 1.0 mL of ODE was added. Finally, the solutions of the Zn and the Se precursors were mixed with each other by stirring, and they were delivered in a microcapillary using a syringe pump. The flow rate was changed from 5 to 25 μLmin^{-1}. The polytetrafluorethylene (PTFE) microcapillary with 500 μm inner diameter was connected from the syringe to an outlet via the reaction part. The reaction part was heated by an oil-bath at 200–240 °C, and the length of the heating zone in the microtube was around 20 cm. The prepared ZnSe QDs were collected and dispersed in hexane or chloroform, and they were purified by precipitation with addition of methanol and acetone.

Results and Discussion

For the continuous-flow synthesis using a microreaction system, precursors should be prepared in liquid form. By dissolving the Zn acetate powder in OLA around 170 °C, solution-type Zn complexes like gel were formed. In the case of Se precursors, the Se powder was dissolved in TBP solution. The continuous-flow microreaction system was set up as illustrated in Figure 1a. After mixing Zn and Se precursor' solutions by stirring, they were moved into the microchannel using a syringe pump. The mixture solution passed through an oil bath which is for heating zone where the nucleation and growth of ZnSe QDs occurred. Figure 1b shows the UV/VIS absorption spectra of aliquots of ZnSe QDs. In order to have a precise determination of the energy position of the absorption edge, one can take the edge position to be determined by the maximum of the first derivative of the optical absorption with respect to the energy and it corresponds to the optical bandgap.[15] As the flow rate decreased from 25, 15, 10, 5 μLmin^{-1}, the QDs' optical bandgap moved to 3.14 eV (394.5 nm), 3.11 eV (398.5 nm), 3.04 eV (408.0 nm), 3.01 eV (412.5 nm), respectively. In Figure 1c, the PL spectra of the purified ZnSe QDs' solution are shown. The impurity emission (asymmetric emission around 390 nm) from not-reacted precursors or Zn complexes disappeared, so the emission from ZnSe QDs was seen clearly. As the flow rate decreased from 25, 15, 10, 5 μLmin^{-1}, the QDs' emission peaks moved to 413, 415, 422, 432 nm, respectively. The faster the flow rate, the shorter the retention time for the growth of QDs. Therefore, the QDs became smaller, so the absorption and emission peaks moved to a shorter wavelength due to a quantum size effect (QSE).

[z]E-mail: dyj@kaist.ac.kr

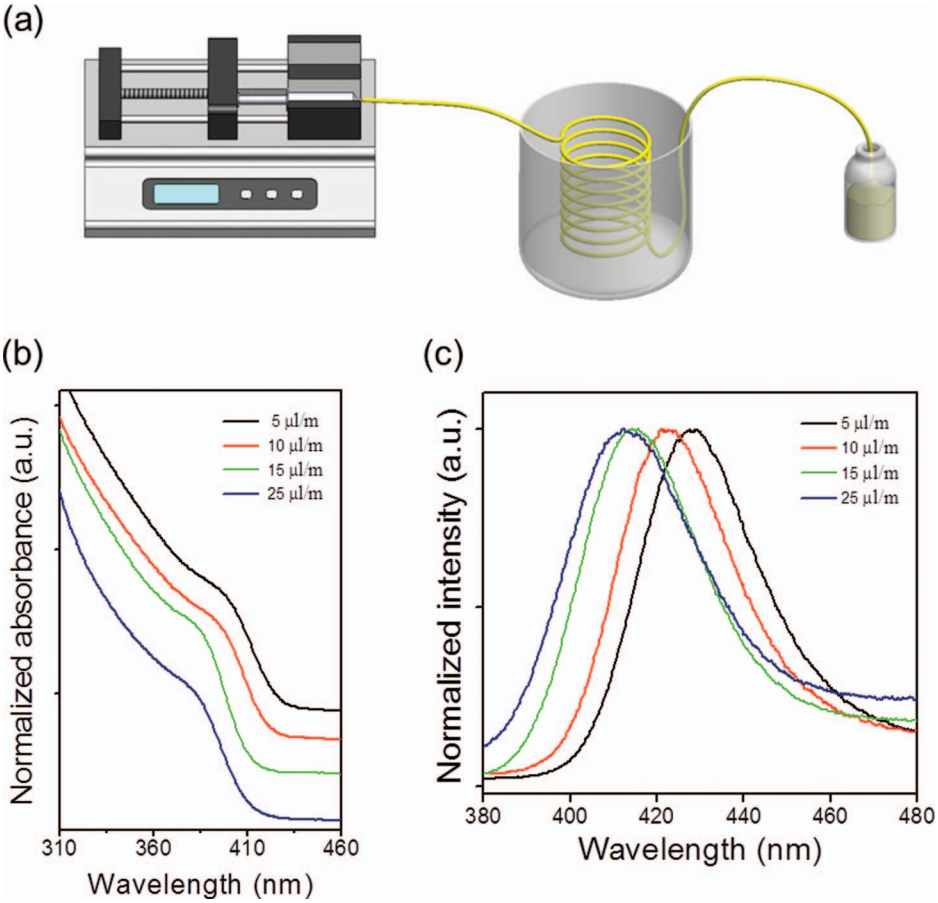

Figure 1. (a) Schematic illustration of a continuous-flow microreactor system for the synthesis of ZnSe QDs, (b) UV/VIS absorption and (c) PL spectra of ZnSe QDs (aliquots) with different flow rate.

Figure 2a shows X-ray diffraction (XRD) patterns of ZnSe QDs. The main diffraction peaks appeared at around 27.2°, 45.2°, 53.6° corresponding to (111), (220), and (311) planes of ZB phase of ZnSe (JCPDS Card No. 65–9602).[10,16] More specifically, the (111) peak of ZB ZnSe was asymmetrically broadened by the convolution of the (100), (002), and (101) peaks of WZ phase of ZnSe (JCPDS Card No. 15–0105). In addition, the suppression of the (102) and (103) planes of WZ ZnSe can be explained by the presence of stacking faults along the (002) direction.[16] The broadening of the peaks is due to the nanosized crystalline domains. Figure 2b and 2c show transmission electron microscopy (TEM) images of ZnSe nanoparticles. They revealed highly crystalline nanostructure with both spherical and rod-shape morphology. In the case of nearly spherical ZnSe QDs (Figure 2b), the size was around 2–3 nm and the measured interplanar spacing (3.28 Å) matched the (111) plane of ZB ZnSe phase. In anisotropic nanostructures (Figure 2c), the diameter was similar to that of the spherical particles but the length was elongated to 5–6 nm. Their interplanar spacing was around 3.53 Å, which was matched with the (100) plane of WZ ZnSe phase. In our continuous microfluidic reaction system, the monomer concentration was fixed and reaction time was long enough due to slow flow rate of precursor solutions. In the initial part of the reaction, high monomer supersaturation kinetically favored both nucleation and growth of the ZB phase, which was more symmetrical than the WZ phase.[16] As the amount of ZnSe QDs synthesized in the microreactor increased, the monomer concentration became extremely low. In the very low supersaturation condition promoting thermodynamic control of the growth, it is expected that the secondary WZ phase growth onto the QDs' surface become dominant. Due to that, stacking faults were observed in these structurally heterogeneous nanostructures (Figure 2c). Therefore, ZB ZnSe QDs and rod-shape nanocrystals with both the WZ and ZB structure coexisted. The selective area electron diffraction (SAED) pattern (Figure 2d) of

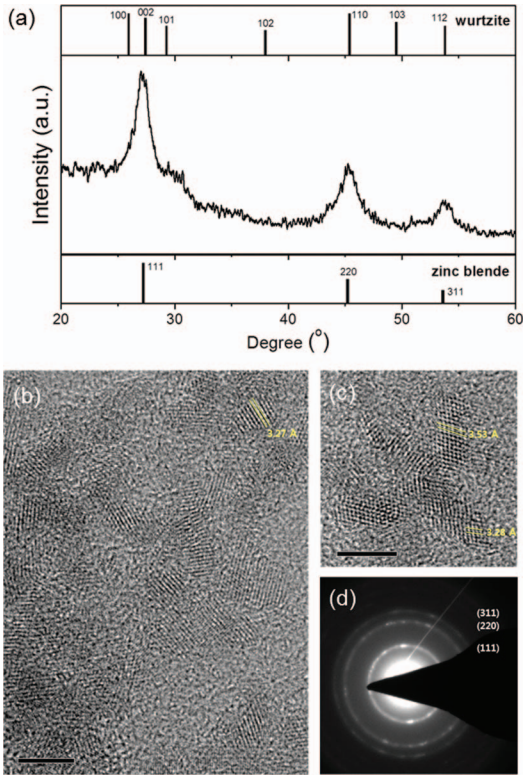

Figure 2. (a) XRD patterns of ZnSe QDs, (b) Low magnification TEM image of ZnSe NPs, (c) High magnification TEM image of rod shape ZnSe nanostructures, (d) SAED pattern of ZnSe QDs. Scale bar of inset is 5 nm.

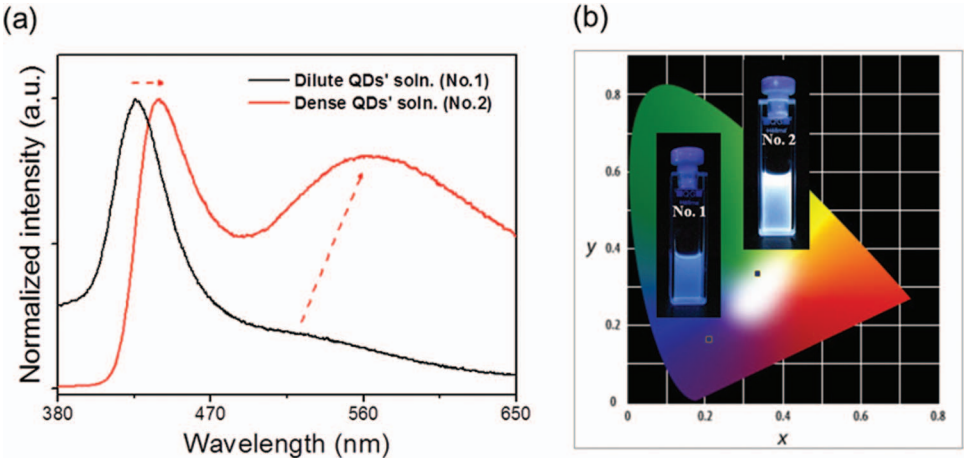

Figure 3. (a) PL spectra of dilute and dense QDs' solution excited at 330 nm, (b) CIE color coordinates and the photos of samples.

the sample was consistent with the ZB ZnSe phase with ring patterns, which is also consistant with XRD patterns (Figure 2a).

Figure 3a shows the PL spectra of ZnSe QDs' solution with the same flow rate (10 μL min^{-1}) and different concentration (dilute and dense QDs' solution). Aliquots of ZnSe QDs were dispersed in 8.0 mL (dilute solution) and 0.5 mL (dense solution) of chloroform. In the dilute solution, the emission was composed of both strong band-edge emission (426.4 nm) and weak defect emission (~522.0 nm). The greenish emission band was ascribed to radiative deep levels generated by strained lattices or crystal imperfections at the surface such as dislocations and vacancies.[17,18] As shown in the TEM image (Figure 2c), it is confirmed that elongated particles have the highly defective crystalline nanostructures. On the other hand, in the dense solution, the band-edge emission exhibited at 440.0 nm, which was red-shifted by 13.6 nm compared to the dilute solution. In addition, the green-yellowish emission band from deep levels (~565.0 nm) increased significantly. Figure 3b shows the Commission Internationale de I′Eclairage (CIE) color coordinates and camera images of ZnSe QDs' solution with different concentration. Sample No. 1 is dilute solution emitting blue light with the CIE value of (0.21, 0.17). Sample No. 2 is dense solution emitting white light with the CIE value of (0.33, 0.33).

Figure 4a shows time-dependent photoluminescence (TDPL) decay measurements for the samples (used in Figure 3) measured at the exciton peak maximum (426.0 nm and 440.0 nm of the dilute and dense QDs' solution). The decay curves of the ZnSe QDs' solution with both low and high concentration were not mono-exponential, and they were fitted by two exponentials: the dilute solution ($\tau_1 = 0.52$ ns, $\tau_2 = 3.16$ ns) and the dense solution ($\tau_1 = 0.99$ ns, $\tau_2 = 4.43$ ns). The longer decay times (τ_2) are interpreted as the intrinsic transition of the QDs or "excitonic transition".[19] The shorter decay times (τ_1) could be partial quenching of the exciton luminescence by surface and lattice defects such as unsaturated surface bonds of Zn or Se, and/or Se vacancies inside the QD, providing additional decay channel.[17,18] The decay curve of the dense solution shows a slower decrease in normalized emission intensity than that of the dilute QDs' solution. This is attributed to Föster resonance energy transfer (FRET) that relates the efficiency of ET from donor-acceptor dipole-dipole interactions to the spectral overlap of donor emission and acceptor absorption.[20–22] Figure 4b exhibits schematic diagram of resonant ET process from small (donor) to large (acceptor) ZnSe QDs. Assuming the ET via a dipole-dipole interaction within a donor-acceptor distance (R), the ET rate scales with R^{-6} dependence.[20–22] In the case of dense QDs' solution, the spatial distance between the individual particles is sufficiently short, so the inter-QD ET occurs efficiently. Furthermore, there was spectral overlap of the donor emission and the acceptor absorption, which increased the ET. Although the energy of excitonic emission transferred sequentially from the small QDs to the large QDs, the energy of defected-related emission does not migrate because the defect in QDs acts as a trap. Therefore, the red-shifted excitonic emission, increased intensity of defect emission, and prolonged decay time in the dense QDs' solution confirms that the energy is transferred efficiently between QDs.

In summary, we first demonstrated white-emitting ZnSe QDs by a continuous-flow microreaction method. The emission from the QDs moved from 413 nm to 432 nm when its flow rate was changed from

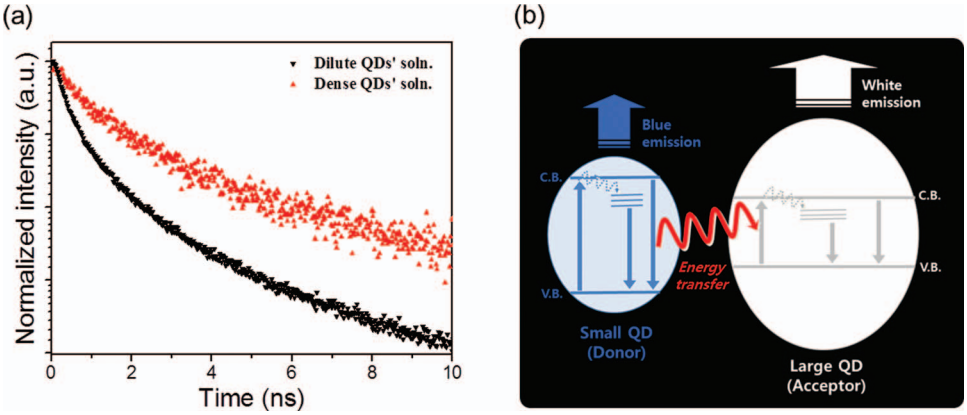

Figure 4. (a) TDPL decay of dilute and dense QDs' solution monitored at 425 nm and 440 nm, (b) Schematic diagram of ET process from small to large QDs in dense QDs' solution.

25 μLmin^{-1} to 5 μLmin^{-1}. The ZnSe QDs had strong band-edge emission and weak defect emission. In dense solution of ZnSe QDs, it showed red-shifted (14.6 nm) band-edge emission and enhanced green-yellow emission from deep levels due to the inter-QD energy transfer comparing with dilute solution, thereby it exhibited white color with CIE color coordinates of (0.33, 0.33). This work related to the ET between individual QDs will become the foundation for advanced QD-based application.

Acknowledgment

This research was supported by WCU (World Class University) program through the Korea Science and Engineering Foundation funded by the Ministry of Education, Science, and Technology.

References

1. A. P. Alivisatos, *J. Phys. Chem.*, **100**, 13226 (1996).
2. W. Liu, M. Howarth, A. B. Greytak, Y. Zheng, D. G. Nocera, A. Y. Ting, and M. G. Bawendi, *J. Am. Chem. Soc.*, **130**, 1274 (2008).
3. D. GeiBler, L. J. Charbonniere, R. F. Ziessel, N. G. Butlin, H.-G. Lohmannsroben, and N. Hildebrandt, *Angew. Chem. Int. Ed.*, **49**, 1396 (2010).
4. M. J. Anc, N. L. Pickett, N. C. Gresty, J. A. Harris, and K. C. Mishraa, *J. Solid State Sci. Technol.*, **2**, R3071 (2013).
5. P. V. Kamat, *J. Phys. Chem. C*, **112**, 18737 (2008).
6. J. J. Choi, Y.-F. Lim, M. B. Santiago-Berrios, M. Oh, B.-R. Hyun, L. Sun, A. C. Bartnik, A. Goedhart, G. G. Malliaras, H. D. Abruna, F. W. Wise, and T. Hanrath, *Nano Lett.*, **9**, 3749 (2009).
7. P. Reiss, M. Protiere, and L. Li, *Small*, **5**, 154 (2009).
8. A. J. deMello, *Nature*, **442**, 394 (2006).
9. S. Krishnadasan, R. J. C. Brown, A. J. deMello, and J. C. deMello, *Lab Chip*, **7**, 1434 (2007).
10. B.-H. Kwon, K. G. Lee, T. J. Park, H. Kim, T. J. Lee, S. J. Lee, and D. Y. Jeon, *Small*, **8**, 3257 (2012).
11. J. Baek, P. M. Allen, M. G. Bawendi, and K. F. Jensen, *Angew. Chem. Int. Ed.*, **50**, 627 (2011).
12. P. Reiss, *New J. Chem.*, **31**, 1843 (2007).
13. N. Pradhan, D. Goorskey, J. Thessing, and X. Peng, *J. Am. Chem. Soc.*, **127**, 17586 (2005).
14. B.-H. Kwon, H. S. Jang, H. S. Yoo, S. W. Kim, D. S. Kang, S. Maeng, D. S. Jang, H. Kim, and D. Y. Jeon, *J. Mater. Chem.*, **21**, 12812 (2011).
15. A. Umar, M. Abaker, M. Faisal, S. W. Hwang, S. Baskoutas, and S. A. Al-Sayari, *J. Nanosci. Nanotechnol.*, **11**, 3474 (2011).
16. P. D. Cozzoli, L. Manna, M. L. Curri, S. Kudera, C. Giannini, M. Striccoli, and A. Agostiano, *Chem. Mater.*, **17**, 1296 (2005).
17. H. S. Chen, S. J. J. Wang, C. J. Lo, and J. Y. Chi, *Appl. Phys. Lett.*, **86**, 131905 (2005).
18. Z. Deng, F. L. Lie, S. Shen, I. Ghosh, M. Mansuripur, and A. J. Muscat, *Langmuir*, **25**, 434 (2009).
19. Ch. Rajesh, A. D. Lad, A. Ghangrekar, and S. Mahamuni, *Solid State Commun.*, **148**, 435 (2008).
20. S. A. Crooker, J. A. Hollingsworth, S. Tretiak, and V. I. Klimov, *Phys. Rev. Lett.*, **89**, 186802 (2002).
21. C. R. Kagan, C. B. Murray, and M. G. Bawendi, *Phys. Rev. B*, **54**, 8633 (1996).
22. U. T. D. Thuy, P. T. Thuy, N. Q. Liem, L. Li, and P. Reiss, *Appl. Phys. Lett.*, **96**, 073102 (2010).